8 July 2024
kreftaprywatny@gmail.com

Multi-bunch and Multi-burst Longitudinal Beam Observation in the PS

D. Krefta, A. Huschauer, A. Lasheen, H. Pahl, G. Trad
CERN, CH-1211 Geneva, Switzerland

Keywords: Beam Quality Monitoring, Performance Monitoring, Longitudinal Tomography

Summary

A new wall current monitor was installed in the PS during the Year-End Technical Stop 2022-2023 with the aim of using it as a longitudinal beam quality monitor. In this note, recent developments concerning the implementation of longitudinal beam observation are presented. The current setup allows us to acquire data from 2 different acquisition channels with 8 different timing bursts in the same cycle. To take advantage of this possibility, a new operational application was developed in Python. It allows the operator or beam physicist to change settings of each burst of triggers and perform a multi-bunch tomography on the acquired data. This increases the amount of available data, speeds up the acquisition process, and prepares the foundation for future automated tomography and online beam quality monitoring.

Contents

1 Introduction

An additional Wall Current Monitor (WCM) was installed in the PS straight section 98 during Year-End Technical Stop (YETS) 2022-2023 [1]. Two WCMs of identical specifications are currently operational in straight section 03 of the PS and have been used for longitudinal observation for the last decade [2]. They replaced the previous WCM in PS installed in 1993. The original motivation for the new WCMs was to build a Longitudinal Beam Quality Monitor (BQM) in the PS, as it already exists in the SPS. The main goal of the SPS BQM is to avoid injecting a beam with poor longitudinal quality into the LHC, by interlocking the beam production. The PS would benefit from a separate BQM to independently analyse the beam quality during the beam preparation phase and routine operation, limiting the injection of out-of-specification beams into the SPS.

The WCM is based on the principle that the particle beam circulating in the vacuum chamber induces a circulating image current in the chamber. This effect allows non-invasive and continuous measurement of the longitudinal beam profile. Based on that acquisition, the longitudinal phase space can be reconstructed by applying longitudinal tomography [3].

In general, the many different PS users have strict requirements on beam quality, but with different emphasis on particular beam characteristics. Applying longitudinal tomography allows obtaining, among others, the emittance and momentum distribution. Nowadays, the Tomoscope application, which is used in the control room, is limited to single-bunch tomography for a single timing in a cycle and a single cycle in the super cycle. The application was written in Java and the GUI and analysis windows are shown in Fig. 1.

To benefit from the newly available infrastructure, an operational application for multi-bunch and multi-burst tomography was developed to measure beam characteristics bunch-by-bunch and at different moments in a cycle. It provides information about the difference in beam parameters between bunches and automatizes the whole process of tomography for multiple bursts [4].

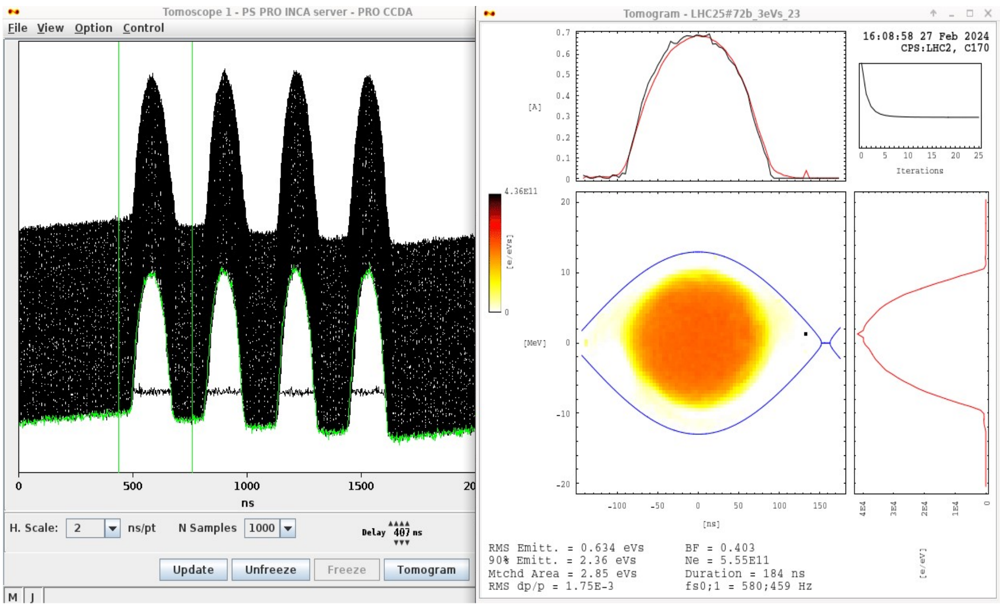

Figure 1: Tomoscope application.

2 Hardware Setup

The WCM98 provides two independent channels, for which new generation acquisition cards compatible with the Open Analogue Signal Information System (OASIS) were installed. Their location is 0152/R-006, and they are inserted in the same rack (BY01.TOM=152) as the hardware used for the operational Tomoscope application. Fig. 2 shows the current setup of the PS WCMs.

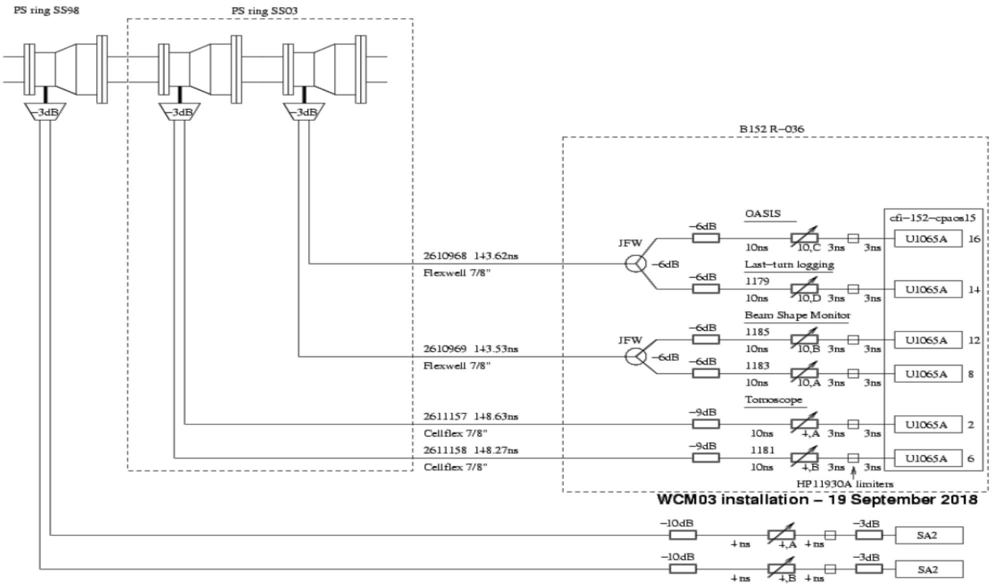

Figure 2: Present cabling scheme for the WCMs installed in Straight Section 98 and 03.[1]

The new cards have tighter constraints in terms of maximum acceptable voltage - 1 V in comparison to the old 10 V, and attenuation must be adapted to avoid damaging the cards. As we can see in Fig. 3, TOF beams generate signals with voltages close to 100 V, while signals for Pb-ion beams can produce voltages lower than 0.1 V. The currently installed attenuation was carefully adjusted to be able to acquire all beam signals ranges by varying the pre-attenuation.

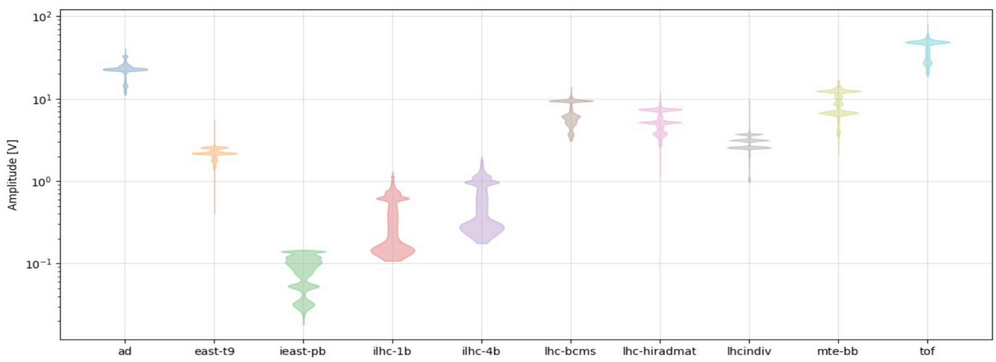

Figure 3: Overview of signal ranges per beam type.

[1]The original drawing was created by J. Belleman and was adapted to include new WCM.

3 Application architecture

A PyQt application was developed to set the acquisition timings, acquire the data from the OASIS cards, perform tomography and provide a GUI for the user in the control room. The data from WCM98 is acquired using the controls infrastructure and post-processed in the application.

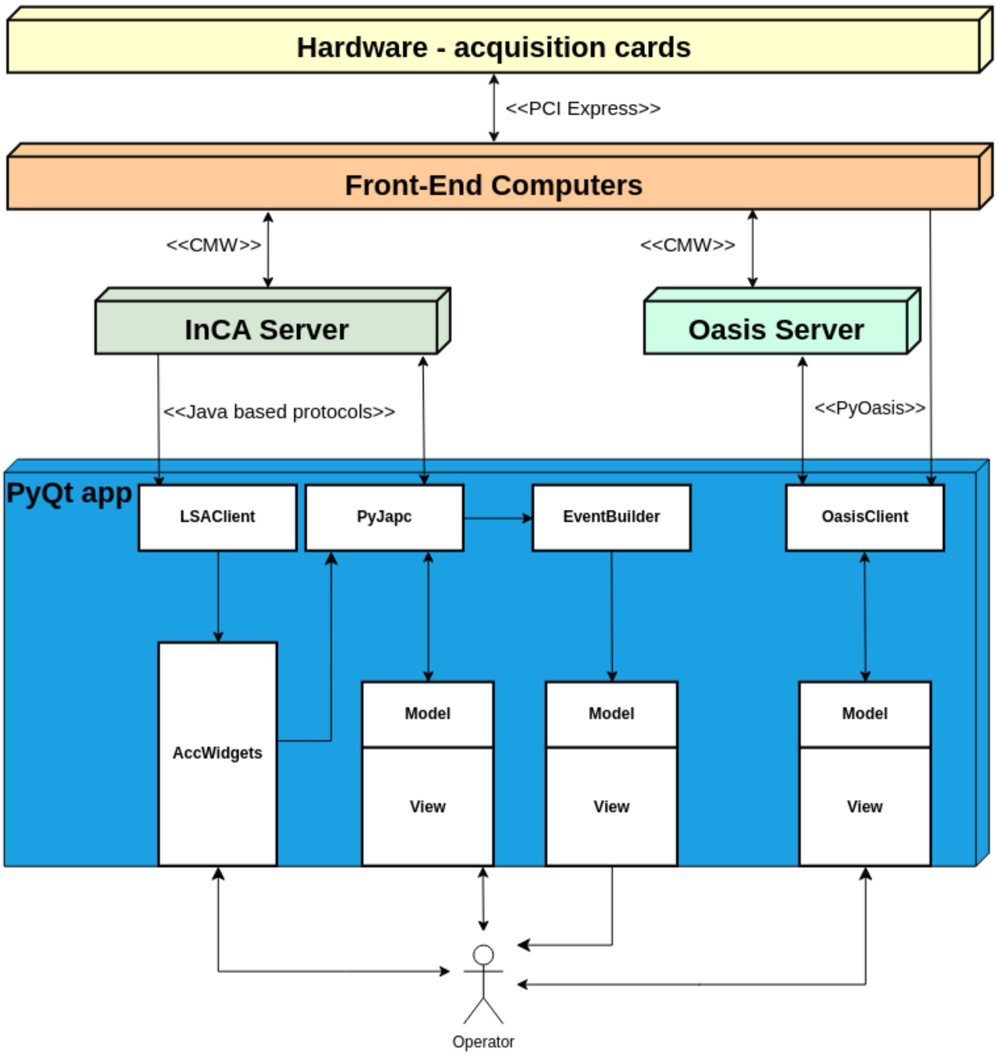

Figure 4: Architecture of the application.

The different building blocks of the architecture shown in Fig. 4 are explained in the following.:

- The front-end computers (FECs), for reliability reasons, are single-board systems without screen, keyboard or hard drive. They only contain a CPU, memory and interfaces (network and bus bridge). To store them, rack-mountable chassis are used. The main purpose of the FECs is to perform the low-level real-time control and acquisition from the accelerator hardware [5].

- The Injector Control Architecture (InCA) provides services for accelerator monitoring and configuration of generic applications. It also uses the LHC Software Architecture (LSA) as a settings manager containing trim history and acquisition core (AcqCore) responsible for acquiring values and postprocessing with enhancing the acquired data [6].

- Controls Middleware (CMW) is the main communication infrastructure responsible for exposing and transporting device data. It includes a family of technologies, such as Remote Devices Access (RDA) and Role-Based Access Control (RBAC). Through CMW, three main operations are available. The first two are the typical command-response operations read (GET) and write (SET). The third operation comes from the publish/subscribe paradigm and is termed SUBSCRIBE [5].

- The OASIS server is a framework for acquisition and processing of analogue signals from devices in the particle accelerators. The signals, which are dispersed throughout the accelerator complex, are digitized by ADC boards sitting in FECs. OASIS provides the Virtual oscilloscope abstraction (Vscope). A Vscope is a software oscilloscope that takes data from different modules and combines them as if they were all connected to the same oscilloscope. This approach makes it possible to observe several signals as if they were next to each other, while they are actually hundreds of meters away from one another [7]. There is also a Java client library available for users to develop their own specific graphical clients [5].

- PyOasis is a high level library that was built for the purpose of this application. It enables access to the OASIS server using Python and allows to create and control virtual scopes.

- PyJapc is the tool to access the CERN accelerator control system in Python using the Java API for Parameter Control (JAPC). With PyJapc we can subscribe to a JAPC parameter, which is a combination of a device name and a device property, according to the Device-property model. Additionally, the field to be worked on can be specified. The JAPC parameter PR.SCOPE15.CH01/Acquisition#value is an illustration of the used convention Device/Property#Field.

- The EventBuilder is a tool used to aggregate data from multiple sources for one specific cycle, ensuring all of them have the same cyclestamp. It is built on top of PyJapc and its design is inferred from the event builder used in UCAP. In the context of the application, it is crucial to have consistent data, especially when some acquisition may be published with some delay or not even acquired at all. All subscribed devices are included in Table 1.

- The model component represents the core logic and data management of an application and is independent of the user interface (view). It encapsulates algorithms and data structures. Primary objectives of the model are to ensure data consistency, integrity, and accuracy. The model handles data storage, retrieval, and manipulation.

- The View pertains to the presentation layer of the application. The manner in which data is presented to users is defined in this component. The view provides a user-friendly interface to interact with the application. Its responsibilities include the design of screens, charts, and visual elements. Furthermore, the view determines formatting, styling, and responsiveness to user input. The view is decoupled from the model, and does not directly manipulate data. An example of such a view is the OasisWidget described in Section 4.2.

Device	**Property**	**Field**	**Meaning**
PR.SCOPE15.CH01	Acquisition	-	WCM Acquisition
PR.BCT-ST	CycleSamples	-	Beam Intensity
PR.BMEAS-B-ST	CycleSamples	-	Magnetic Field
PR.BMEAS-BDOT-ST	CycleSamples	-	Magnetic Field derivative
PA.FREV-SD	CycleSamples	-	Revolution Frequency
PA.VD20-80-SA	CycleSamples	-	Voltage Detected 20MHz in Straight Section 80
PA.VD20-92-SA	CycleSamples	-	Voltage Detected 20MHz in Straight Section 92
PA.VD40-77-SA	CycleSamples	-	Voltage Detected 40MHz in Straight Section 77
PA.VD40-78-SA	CycleSamples	-	Voltage Detected 40MHz in Straight Section 78
PA.VP200-SA	CycleSamples	-	Voltage Programmed 200MHz
PA.GSV20	Enable	enabled	Status of 20MHz cavity
PA.GSHMAIN	Setting	amplitudes	Harmonic main
PA.GSHX	Setting	amplitudes	Harmonic X
PA.GSHY	Setting	amplitudes	Harmonic Y
PA.GSHZ	Setting	amplitudes	Harmonic Z
PA.GSVPSUMX	Setting	amplitudes	Sum of X voltages in 10MHz
PA.GSVPSUMY	Setting	amplitudes	Sum of Y voltages in 10MHz
PA.GSVPSUMZ	Setting	amplitudes	Sum of Z voltages in 10MHz

Table 1: List of parameters, for which data is received using PyJAPC subscriptions.

4 Graphical User Interface

The design of the application GUI is a crucial part of the project. Operators in the control room use several dozen applications. The learning curve in this profession is very steep. Significant effort has been made to create an intuitive application with as low as possible complexity and familiar interface to the well adopted Tomoscope application. The current view of the GUI is visible in Fig. 5. One can distinguish two parts of the application that can be modified by the user (triggering control panel and Oasis control panel) and two visualizations parts (cycle parameters plot and acquisition plot).

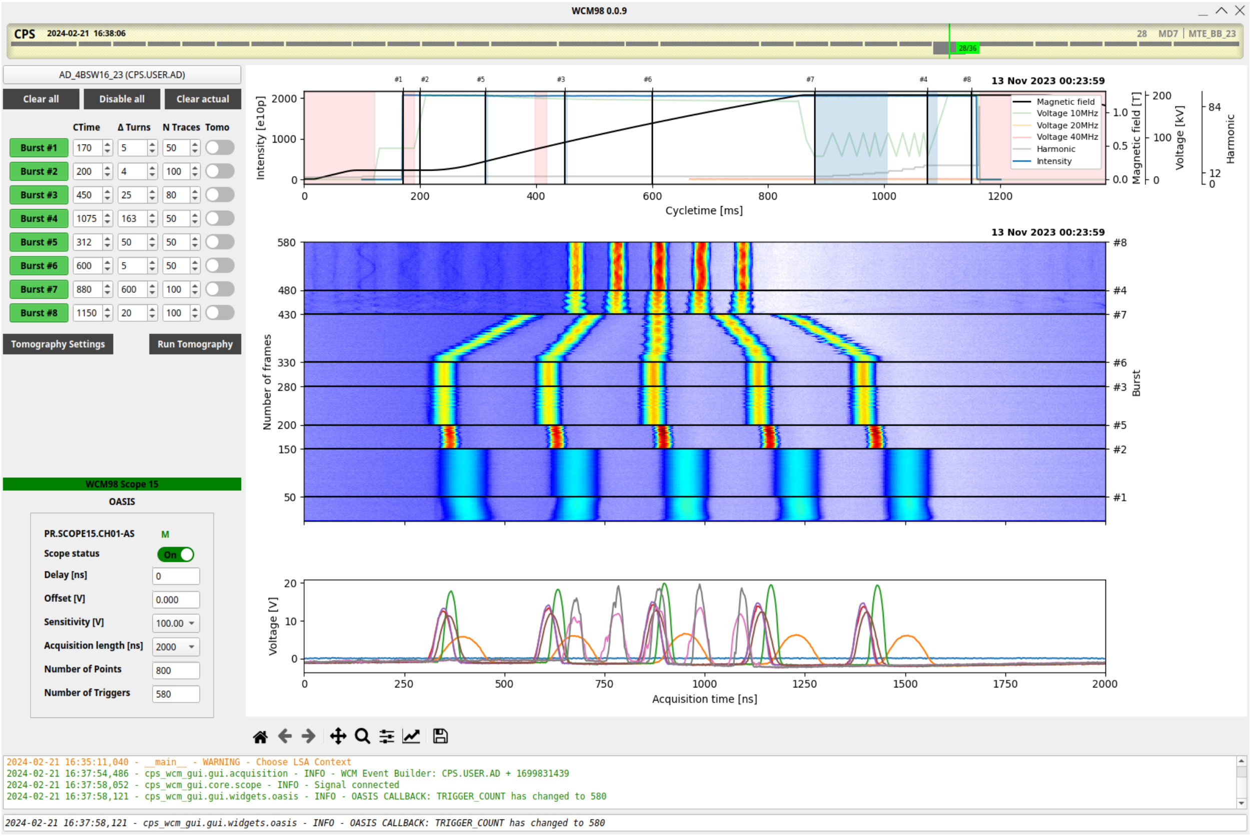

Figure 5: Main window of the application.

4.1 Triggering control panel

It includes a button that is connected with the LSA Selector widget (acc-widget) that allows the user to choose a specific cycle. After clicking, the PyJapc subscription selector is updated. There are 3 additional buttons that are connected with changing multiple settings at once:

- Clear all – turn off all bursts and set every setting ("CTime", "Δ Turns", "N Traces") to 0 for all timing users.
- Disable all – turn off all bursts for all timing users.
- Clear actual – turn off and set every setting to 0 for the current user.

In a grid layout, there are:

- Buttons with burst indices - enable and disable a specific burst.
- Spinboxes "CTime" - time in the cycle when a trigger burst will start acquiring data with 1ms precision.
- Spinboxes "Δ Turns" - turn distance between triggers acquisitions.

- Spinboxes "N Traces" - number of triggers per burst.
- Toggles "Tomo" - enable tomography.

Additional buttons are related to the longitudinal tomography:

- Tomography Settings - opens a window with advanced analysis parameters for tomography.
- Run Tomography - launches the longitudinal phase space reconstruction for the bursts selected using the Tomo toggle.

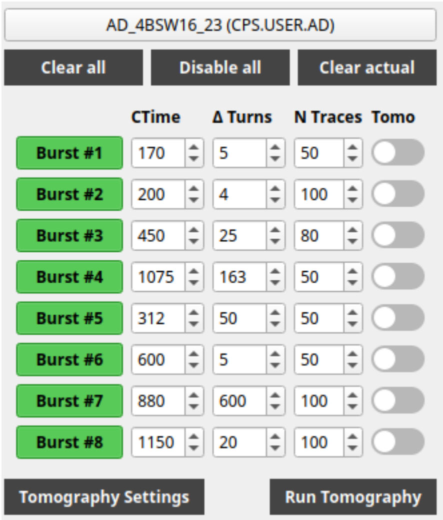

Figure 6: Triggering control panel.

4.2 Oasis control panel

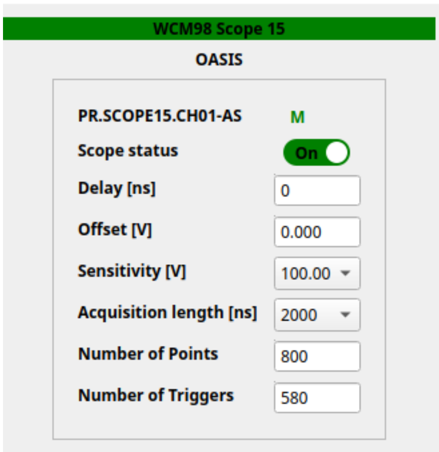

Figure 7: Oasis control panel.

The "WCM98 Scope 15" button in the Fig. 7 creates a virtual scope with predefined settings saved in the configuration file. The button's green color means the virtual scope has been successfully created, otherwise the color is red. The Oasis widget, visible in the framed area, allows controlling the virtual scope in the same way as in the Oasis application, but with a limit to the following seven actions:

- Scope status - indicates whether the virtual oscilloscope is actively acquiring (On) or if it has paused (Off) data acquisition.
- Delay - refers to the adjustable time delay in nanoseconds between the trigger event and the start of the acquisition for all the bursts.
- Offset - this adjustment allows the waveform to be shifted up or down along the vertical axis without changing its shape or the voltage levels of the signal being measured.
- Sensitivity - it represents the sensitivity setting of the vertical axis of the virtual oscilloscope display. The acquisition card has the attenuation of 1V, and the pre-attenuation is always adjusted in the signal path.
- Acquisition length - refers to the duration of time over which the virtual oscilloscope captures and records a single trace.
- Number of points - refers to the total number of sample points acquired and stored for each waveform.
- Number of triggers - count of trigger events that should occur within an acquisition session. This number is automatically updated when the user changes the number of traces in the triggering control panel (Fig. 6), as it is the sum of all number of traces for all active bursts.

The first line provides additional information about the main/secondary status, with the green letter "M" indicating the main status. It is not possible for two users to control the same scope simultaneously. Mastership is assigned based on the priority of the application (e.g., if someone connects to the scope using the dedicated Oasis application and the scope is already in use in our application, it will switch mastership to secondary mode in our application and show main status in Oasis) and the order of connection to the scope (the user who connects first at the same priority level gets mastership). In secondary mode, it is not possible to change the scope's settings, but you can still acquire data with the settings defined by the main user.

It is worth mentioning that at this moment, acquisition cards are limited to a maximum of 10.000.000 points acquired during an acquisition session (number of points multiplied by number of triggers).

4.3 Plot of cycle parameters

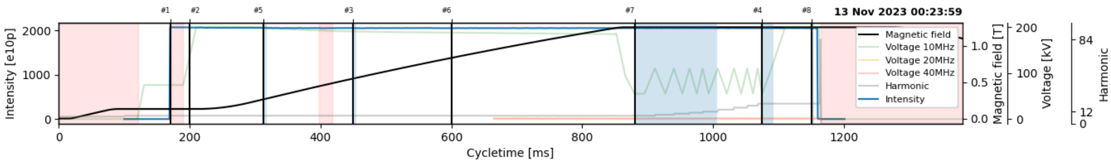

Figure 8: Parameters plot.

The parameters plot (Fig. 8) is a supporting plot to set up the acquisition correctly. It shows intensity, magnetic field, harmonic number and the voltage for 10, 20 and 40 MHz cavities. Subscribed devices behind these parameters are described in Table 1.

Red areas in the plot correspond to the moments when tomography is not possible (no voltage) or not recommended (200MHz blow-up). Black vertical lines correspond to particular bursts timings in the cycle. Blue rectangles, created for all the bursts, show the predicted acquisition time, e.g. Burst#7 in Fig. 8.

Acquisition time prediction is based on the revolution frequency and can be equal to or slightly greater than real acquisition time. It is especially important in case of overlapping bursts - one burst starts acquiring the data before data acquisition for the previous burst finished. It may cause the acquisition to be compromised or not published at all in such a case. With this visualization of predicted acquisition time, the user can be aware of such a situation and adjust the bursts accordingly.

The cycle stamp is displayed in the upper right corner, as it may differ from the time in the acquisition plot (Fig. 9) in the event that the WCM acquisition data is not published during a cycle. The horizontal axis may have different lengths for the purpose of higher resolution, and it is defined as a 1.15 length of non-zero intensity.

4.4 Acquisition plot

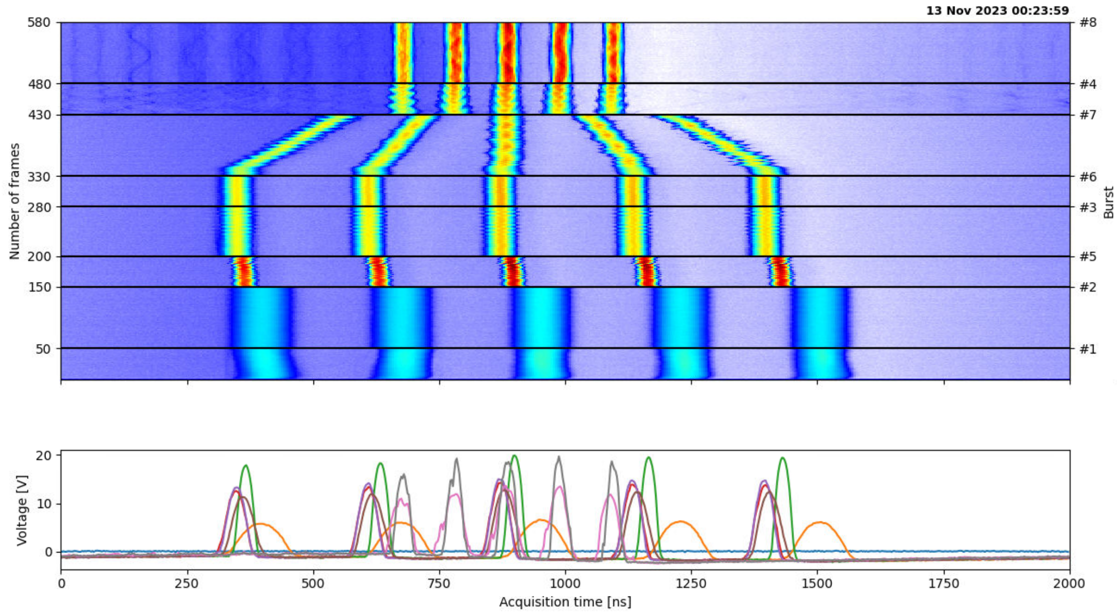

Figure 9: Acquisition plot.

Oasis acquisition data is received using PyJapc in a numpy matrix numeric format. As shown in Fig. 8, it is plotted as a two-dimensional waterfall image, with the color code representing the signal voltage level. With this plot, we can clearly see the evolution of the longitudinal beam profile for the different bursts. In the image, there are visible black, horizontal lines that correspond to the particular bursts timings. The bottom plot shows the first profiles of each burst, which allows us to see the differences in shape and signal voltage.

5 Tomography

Since the Austrian mathematician J. Radon published the proof [8] that any two- (three-) dimensional object can be reconstructed from the set of its one- (two-) dimensional projections, the field of tomographic reconstruction has developed and been used in various domains. Indeed, the English computer engineer Sir G.N. Hounsfield was awarded the Nobel Prize for Medicine in 1979 for his pioneering contribution to computer-assisted tomography. Longitudinal phase space tomography has been adapted to reconstruct the non-linear synchrotron motion at CERN in the PS complex for many years, and it is a highly valuable tool for evaluating the longitudinal characteristics of both operational and machine development beams [3].

The fundamental principle of tomography is to merge the data from a sufficient quantity of N-1-dimensional projections, thereby enabling the reconstruction of a comprehensive N-dimensional image [3], e.g. imaging with medical computed tomography scans. This principle can also be applied to longitudinal particle distributions in synchrotrons to reconstruct the longitudinal phase space.

Particles in a bunch have some distribution in longitudinal phase space, which will rotate due to synchrotron motion. In a WCM, the distribution of the phase space is projected onto the longitudinal axis at different angles as the phase space rotates. Recording the longitudinal profiles on a number of machine turns, suitable for viewing the projection of the distribution from multiple angles, can then be used to perform tomography and reconstruct the longitudinal phase space [3].

Acquiring a sufficient number of one-dimensional profiles from WCM and applying phase space tomography algorithms to them may allow the reconstruction of the longitudinal beam distribution as well as obtaining many important longitudinal parameters.

Longitudinal tomography is performed after clicking the "Run tomography" button in the application. It launches algorithms that were improved and translated into Python [9]. For this purpose, an acquisition must be performed, and the user must have selected for which burst tomography should be done. A bunch detection algorithm is performed for each selected burst. The first profile of each burst acquisition is used to find peaks. A numpy matrix that captures 90% of bucket length centered around each peak (45% to the left and 45% to the right) is used for tomography.

Depending on the number of bunches in each burst acquisition, a different window appears, which shows the output of the tomography in a graphical representation (Fig. 10, Fig. 11).

5.1 Single-bunch tomography

In case of an acquisition with a single bunch the result window (Fig. 10) is similar to the Tomoscope application output that is currently used operationally.

The largest plot is a two-dimensional histogram of the phase space distribution. The two orthogonal projections of the phase space distribution are shown in blue on the top and the right side. The measured profile, for which reconstruction was made, is depicted in orange, subsequent to rebinning factor and scaling, for direct comparison with the projection onto the time axis. Finally, in the upper right-hand corner, a brief plot provides a quantitative assessment of the degree of convergence among the iterations of the reconstruction algorithm. Generally, one would like to see this curve descend to less than a third of its initial value [3].

Several important beam parameters appear on the right side of the plots, summarizing the statistical properties of the distribution. The RMS emittance and RMS momentum spread are both calculations that are weighted by the individual pixel contents.

A foot-tangent algorithm is applied to the leading and trailing edges of the longitudinal profile in order to calculate the duration in ns. The matched area within the matched phase space contour, traversing through both the resulting foot-tangent points [3], is also enumerated. The synchrotron period Ts at the centre of the bucket is calculated. The cycle selector and date of acquisition are also included.

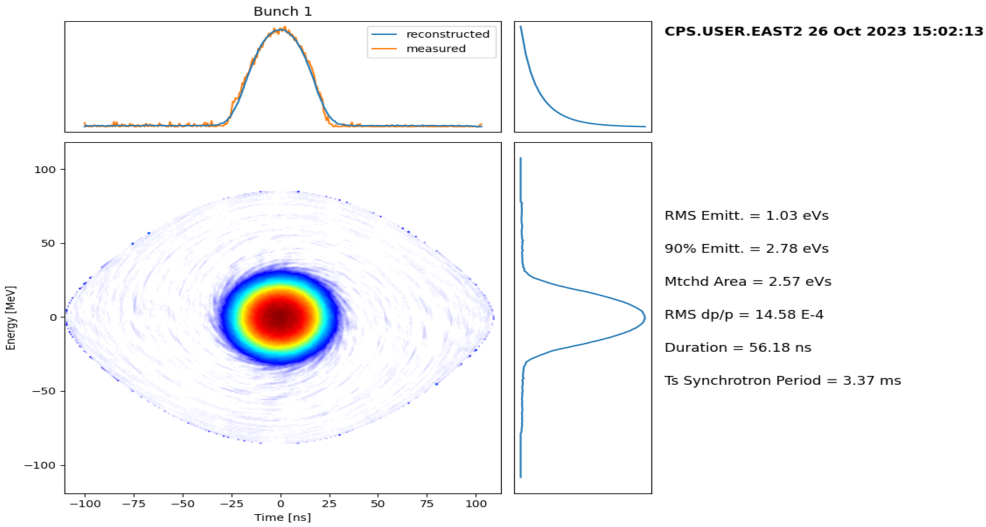

Figure 10: Single-bunch tomography plot.

5.2 Multibunch tomography

When the acquisition of a burst contains more than one bunch, a similar window will be produced as for a single bunch. However, the statistics pertaining to the bunches will be plotted rather than single values, and only the longitudinal phase space reconstruction for the first bunch will be plotted, as shown in Fig. 11. On the right side of the main plot, separate plots for emittance, momentum spread, and bunch length appear, based on the same statistics described in the previous section on the single-bunch tomography. The plots show how the values differ between the bunches. Each chart contains an average value, which is also plotted (dashed line).

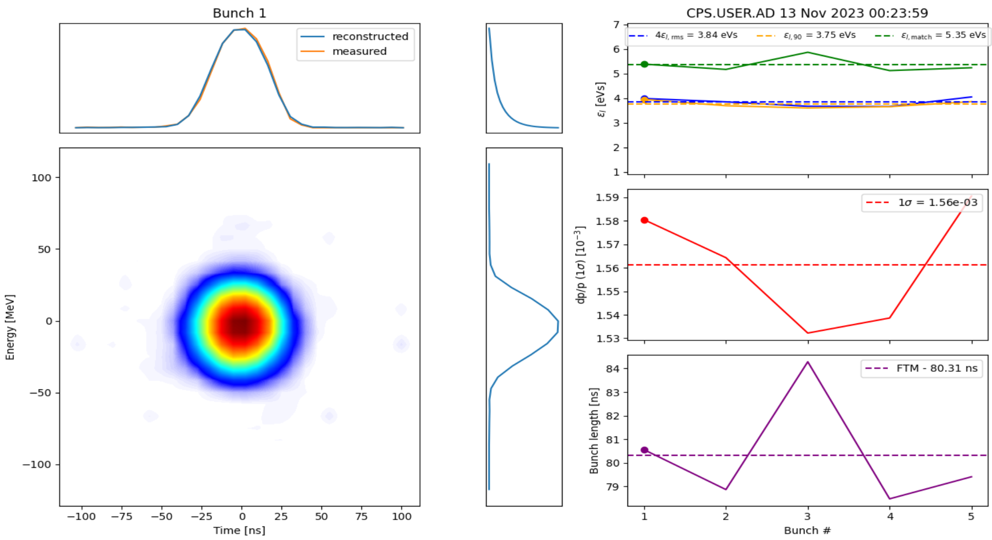

Figure 11: Multi-bunch tomography plot.

6 Summary of new features and ideas for future developments

The new operating application enables users to achieve results comparable to those obtained with the Tomoscope application, while leveraging the capabilities of the new wall current monitor. A primary advantage of the new application is the ability to perform multi-bunch and multi-burst tomography simultaneously, which was not possible in the Tomoscope application. Visualizing burst timings alongside cycle parameters (see Fig. 8) assists operators in planning measurements, eliminating the need to open additional applications for cycle parameter visualization. Within the new application, the OASIS control panel (see Fig. 7) allows users to manipulate the virtual scope using the PyOasis library.

The next step would involve automated tomography and an online beam quality monitor. Algorithms for multi-burst and multi-bunch tomography would be executed for each beam on a dedicated server. Results could be analyzed in real-time and saved in the NXCALS database for future research.

There is still limitation in regard to quality of acquisition for multiple bursts, as we can not yet modify Oasis Scope and Channel settings during the cycle. For instance, the manipulation of sensitivity before and after splitting remains unfeasible, which could enhance the resolution of acquisition.

Furthermore, the bunch detection algorithm could also be improved. Currently, 90% of the bucket length is always used for tomography. While this is a safe and general approach, there could be a separate algorithm for each beam type that allows us to narrow down the acquisition as much as possible to the bunch.

7 Acknowledgements

We extend our heartfelt gratitude to Simon Albright for his invaluable assistance in unravelling the intricacies of tomography, his active involvement in debugging, and his proactive approach throughout. We would like to thank Ole Marqversen for his efforts in installing and diligent testing the new WCM. Our sincere appreciation goes to Dimitris Lampridis for his support and assistance in navigating the new WCM and OASIS application. We express our gratitude to Marcel Coly, Rodolphe Maillet, Mohammad Zishan Ansari, Joseph McCarthy and for their collaborative efforts in shaping the development of the application and rigorous testing. A special thank you to Jean-Francois Comblin for his guidance in understanding the underlying algorithms powering the Tomoscope application. We are deeply grateful to Denis Cotte for LSA Settings definition, which will facilitate automatic loading of configurations for different cycles and Michi Hostettler for generously sharing his extensive knowledge and offering valuable insights.

References

[1] Jeroen Belleman and Bettina Mikulec. PS Beam Quality Monitor - Wall Current Monitor Installation in SS98 of PS Ring. https://edms.cern.ch/document/2783725/1.0. Accessed on 2024-02-27.

[2] JM Belleman, William Andreazza, AA Nosych, and Cerdanyola del Valles. A new wall current monitor for the cern proton synchrotron. *Proceedings of IBIC2016*, 2016.

[3] S Hancock. A simple algorithm for longitudinal phase space tomography. Technical report, CERN, Geneva, 1997.

[4] Pawel Kozlowski. Longitudinal Beam Profile Acquisition with Bursts of Triggers in the CERN Proton Synchrotron. Akwizycja danych podłużnych profili wiazek czastek w akceleratorze Proton Synchrotron w CERN, 2019. Presented 28 Mar 2019.

[5] Stephane Deghaye and Eve Fortescue-Beck. Introduction to the BE-CO Control System. 2020.

[6] G Kruk, S Deghaye, O Kulikova, V Lezhebokov, M Pace, P Pera Mira, E Roux, and J Pawel Wozniak. How to Successfully Renovate a Controls System? - Lessons Learned from the Renovation of the CERN Injectors' Controls Software. 2014.

[7] Dimitrios Lampridis, Tristan Gingold, David Michalik, Aurelien Poscia, Miguel Serans, Mamta Shukla, and Tiago Pereira da Silva. Renovation of the Trigger Distribution in CERN's Open Analogue Signal Information System Using White Rabbit. *JACoW*, ICALEPCS2021:839–846, 2022.

[8] Johann Radon. On the determination of functions from their integrals along certain manifolds. *Mathematisch-Physische Klasse*, 69:262–277, 1917.

[9] Simon Albright, Christoffer Grindheim, Alexandre Lasheen, and Anton Lu. Recent Developments in Longitudinal Phase Space Tomography. *JACoW IPAC*, 2022:347–350, 2022.